第 31卷 第 8期　　焊　接　学　报　　Vol.31　No.8
2010年 8月　　TRANSACTIONS OF THE CHINA WELDING INSTITUTION　　August　2010

激光－MIG复合焊熔透状态评价方法

张永强[1]，　陈武柱[2]，　双元卿[2]，　王康健[2]，　单际国[2]
（1. 首钢集团 技术研究院，北京　100043；2. 清华大学 机械工程系，北京　100084）

摘　要：在有坡口间隙对接焊时，焊缝根部成形状态是衡量复合焊搭桥质量及其适应能力的重要指标．提出了以背面相对熔宽作为 CO_2 激光－MIG复合焊熔透状态的定量评价指标，并以此为依据将熔透状态分为未熔透、适度熔透和过熔透，其中适度熔透是最佳的熔透状态．基于相对熔宽的评价指标，研究了工艺参数及坡口间隙变化对熔透状态的影响规律；通过调节激光功率、焊接电流或焊接速度增加热输入，都可使背面相对熔宽增大，从而改变熔透状态；随着坡口间隙的增大，熔透状态从未熔透过渡到适度熔透，再过渡到过熔透．

关键词：激光复合焊；评价指标；熔透状态；背面相对熔宽
中图分类号：TG456.7　文献标识码：A　文章编号：0253－360X（2010）08－0041－04

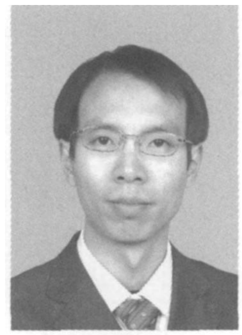

张永强

0　序　　言

激光电弧复合焊是指将激光和电弧这两种不同的热源耦合共同作用于同一区域，从而综合了两种热源的优点，并避免了各自缺陷的焊接方法[1]．相对于传统的单一热源，复合焊具有熔深大、速度快、稳定性高、允许的坡口间隙大、气孔少等特点[2]，在汽车、造船、起重机械等领域得到了越来越广泛的应用[3－5]．

作为激光焊的重要补充和发展，激光电弧复合焊对激光焊的最大优势就是良好的坡口间隙桥接能力．尽管如此，对坡口间隙桥接后能否保证良好的焊缝成形，仍然是激光电弧复合焊首先要关注的问题．对对接焊来说，衡量焊接成形质量的最重要指标是焊缝的熔透状态，一般要求完全熔透，不允许未熔透和过熔透．

焊接过程中，评价焊缝成形的主要参数有焊缝正面熔宽、余高、焊缝熔深等，在熔透时有焊缝背面熔宽、背面余高等．在激光－MIG对接复合焊中，目前国内外学者主要集中于对前者（正面熔宽、余高、熔深）的研究，对熔透状态（是否熔透、熔透后反面成形情况）的研究却很少涉及到．为定量衡量激光－MIG复合焊的熔透状态，文中提出了相对熔宽的质量评价指标，并且基于相对熔宽研究了工艺参数及坡口间隙变化对熔透状态的影响规律．

收稿日期：2009－02－26
基金项目：国家自然科学基金资助项目（50175061）

1　复合焊熔透状态的评价指标

背面熔宽反映了熔池液体金属到达工件背面的成形情况，但当接头间隙变化时，它还不能准确反映工件对接根部的熔合程度．图 1中虚线表示试板间隙，实线表示熔合线，其中图 1b示意了背面间隙由小变大、熔宽恒定的情况．从图 1b中可以看出，背面熔宽无法准确地反映熔透状态的变化．

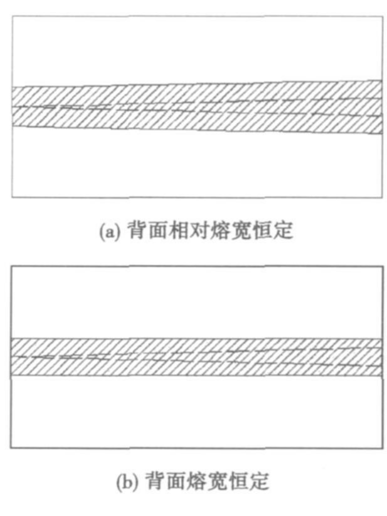

(a) 背面相对熔宽恒定

(b) 背面熔宽恒定

图 1　变间隙熔透状态评价指标比较
Fig. 1　Comparison of different evaluation criterion

考虑到激光－MIG复合焊可以大大降低对工件加工和装配的要求，所以其焊接对象往往对接间隙

变化较大. 为了适应这种情况, 文中提出在激光－MIG复合焊时, 以背面相对熔宽作为评价其熔透状态的指标, 即

$$R_w = W - d$$

式中: R_w为背面相对熔宽; W为背面熔宽 (绝对熔宽); d为焊前坡口间隙.

如图 2所示, 背面相对熔宽反映了对焊缝根部两侧工件熔合的程度, 是考虑了接头间隙宽度后的熔透状态, 如图 1a所示可以定量描述熔透状态的变化.

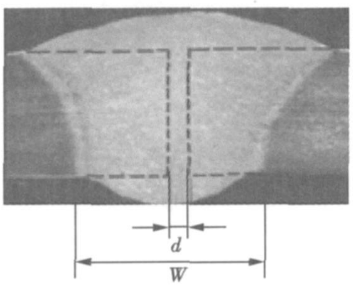

图 2 背面相对熔宽
Fig. 2 Relative root width of weld

在对接复合焊中, 随着工艺参数的不同, 焊缝熔透状态也发生变化. 通过大量焊接试验和焊缝背面熔透状态的观察和分析, 对于 3 mm厚材料, 熔透状态根据背面相对熔宽 R_w的大小可以分为三类.

1.1 未熔透

未熔透缺陷: $R_w < 0$. 焊接过程中金属液体未完全达到工件间隙的下表面, 工件下表面没有完全熔合, 焊后在焊缝背面看到明显的凹陷. 如图 3a所示, 激光功率 1.2 kW, 焊接电流 60 A, 焊接速度 12 mm/s, 当坡口间隙小于 0.1 mm时, 就会出现这种状态. 由于未能将背面间隙填满, 这是一种很明显的未熔透的缺陷.

不稳定的熔透状态: $R_w < 0.5$ mm. 截面如图 3b采用激光功率为 1.2 kW, 焊接电流 60 A, 焊接速度 12 mm/s的焊接工艺参数, 坡口间隙为 0.2 mm时, 焊接过程中, 金属液体正好达到工件下表面, 而且也填满间隙, 但背面熔宽 W与间隙 d相差不大, 导致背面相对熔宽 R_w很小, 焊缝背面也几乎没有余高, 这种状态虽然也接近熔透, 但因背面相对熔宽 R_w较小, 焊接条件稍有波动则焊缝根部不能完全熔合, 熔透不稳定, 因此属于一种不稳定的熔透状态, 同样归为未熔透.

1.2 适度熔透

0.5 mm ≤ R_w ≤ 2 mm. 截面如图 3c, d所示, 焊接工艺参数为激光功率 1.2 kW, 焊接电流 60 A, 焊接速度 12 mm/s, 坡口间隙 0.25～0.7 mm; 或激光功率 2 kW, 焊接电流 120 A, 焊接速度 15 mm/s, 坡口间隙 0.3～0.8 mm. 焊接过程中, 焊缝根部熔合良好, 正反面成形俱佳, 背面余高合适, 背面相对熔宽大小均匀适度, 熔透充分.

1.3 过熔透

$R_w > 2$ mm. 焊缝截面如图 3e所示, 焊接工艺参数为激光功率 2 kW, 焊接电流 120 A, 焊接速度 15 mm/s, 坡口间隙 > 0.85 mm时进入过熔透状态. 此时由于焊接过程热输入过大, 金属熔化量多, 导致焊缝背面凸起严重, 背面熔宽、背面相对熔宽、背面余高均明显大于适度熔透. 过熔透状态下存在焊缝热影响区大, 工件变形严重等问题, 而且背面余高过高也易导致应力集中的缺陷, 严重时产生明显的塌陷, 如图 3f所示, 背面余高甚至已经大于工件厚度; 进一步增大坡口间隙, 会出现焊穿缺陷 (图 3g).

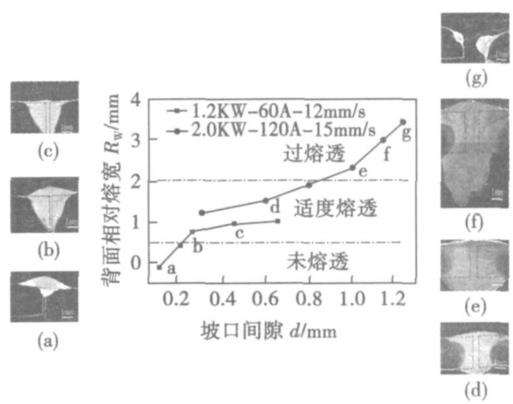

图 3 熔透状态的类型
Fig. 3 Different kinds of penetration statuses

上述三种熔透状态中, 以适度熔透状态最佳, 熔透稳定, 焊缝成形均匀美观. 在焊接过程中, 为获得适度熔透状态, 需要合理选择复合焊工艺参数, 但由于激光－MIG复合焊涉及的工艺参数较多, 包括激光功率、焊接电流、焊接速度、坡口间隙等, 如何确定各参数对熔透的影响, 保证整条焊缝都处于适度熔透状态, 这对指导实际应用具有重要意义.

2 试验装置和材料

试验装置如图 4所示, 激光器采用 PRC3000快轴流 CO_2激光器, 光束模式为 $TEM_{00} + TEM_{01}$, 最大输出功率为 3 kW; 激光采用反射镜聚焦, 焦距为 190 mm. 电弧焊机为松下 YD—350AG2, 可输出脉冲电流, 平均电流 40～350 A, 焊丝直径 1.2 mm. 焊炬采用自制的复合焊焊炬, 实物如 4b所示. 焊接过

程中激光光轴垂直工件表面, MIG焊炬轴线和工件夹角约为 60°, 采用激光先行的方式. 工件为 3 mm厚不锈钢, 大小为 200 mm× 50 mm, 表面经过砂纸打磨和丙酮擦拭. 采用 I型坡口对接的焊接方式.

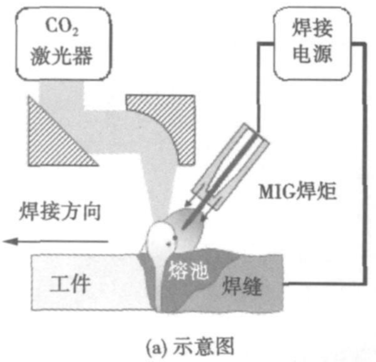

图 4 复合焊试验装置示意及实物图

Fig. 4 Schematic diagram and picture of CO_2 laser-MIG hybrid welding equipment setup

3 试验结果

背面相对熔宽是评价熔透状态的主要指标, 下面在激光 —电弧距离均固在一较佳值 (此处取 2 mm)条件下, 研究激光功率、MIG焊接电流、焊接速度、坡口间隙对背面相对熔宽的影响.

固定其余参数不变, 改变激光功率, 观察激光功率对焊缝背面成形的影响. 图 5是焊接电流 80 A, 焊接速度 10 mm/s情况下, 焊缝背面熔宽和背面相对熔宽随激光功率的变化曲线, 图中横坐标表示激光功率, 左边的纵坐标表示背面熔宽, 右边的纵坐标表示背面相对熔宽, 根据背面相对熔宽的大小, 可以划分出三种熔透状态: 未熔透、适度熔透和过熔透. 在坡口间隙为 1 mm时, 随着激光功率增大, 背面熔宽逐渐增大, 背面相对熔宽也随之增大, 焊缝逐渐从未熔透向适度熔透状态转变, 再变化到过熔透.

图 6是在间隙为 1 mm, 激光功率 2 kW, 焊接速

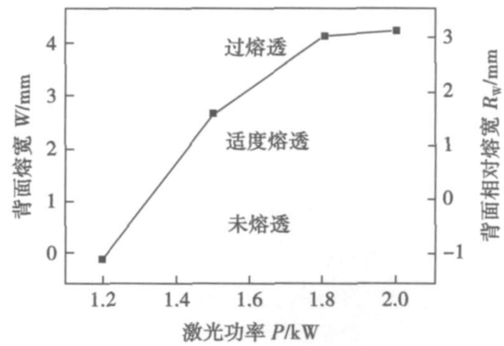

图 5 背面熔宽和背面相对熔宽随激光功率的变化

Fig. 5 Variation of relative root width of weld with laser power

度 15 mm/s时, 背面熔宽和背面相对熔宽随焊接电流变化的情况. 图中横坐标表示焊接电流, 左右纵坐标分别为背面熔宽和背面相对熔宽的大小, 同样根据背面相对熔宽的大小划分出三个熔透状态. 从图 6中可以看到, 随着焊接电流的增大, 熔透状态由开始的未熔透过渡到适度熔透, 再过渡到过熔透.

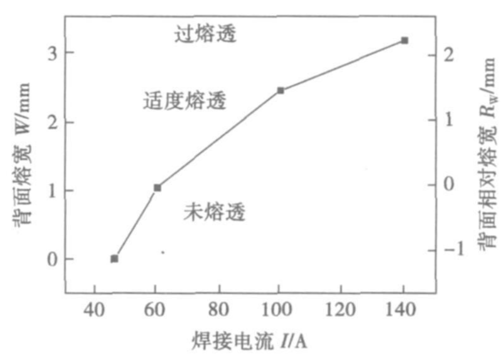

图 6 背面熔宽和背面相对熔宽随焊接电流的变化

Fig. 6 Variation of relative root width of weld with arc current

焊接速度的改变, 意味着激光热输入和电弧热输入的同时改变. 图 7是间隙为 1 mm, 激光功率 2 kW时背面熔宽和背面相对熔宽随焊接速度变化的情况. 图中横坐标表示焊接速度, 左右纵坐标分别为背面熔宽和背面相对熔宽的大小, 同样根据背面相对熔宽的大小划分出三个熔透状态. 从图 7中可以看到, 随着焊接速度的增大, 复合焊背面熔宽和背面相对熔宽都随之减小.

图 8为焊接电流为 140 A, 焊接速度为 15 mm/s, 激光功率为 1.2, 1.5, 1.8, 2.0 kW时, 背面相对熔宽随着坡口间隙的变化情况. 从图 8中可以观察到, 背面相对熔宽随着坡口间隙的增大而增大.

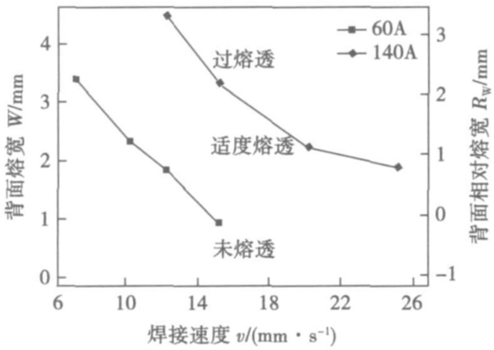

图 7 背面熔宽和背面相对熔宽随焊接速度的变化

Fig. 7 Variation of relative root width of weld with welding speed

激光功率为 1.2 kW时,熔透状态从未熔透向适度熔透转变;激光功率为 1.5,1.8,2.0 kW时,随着间隙的增大,熔透状态从适度熔透向过熔透转变.

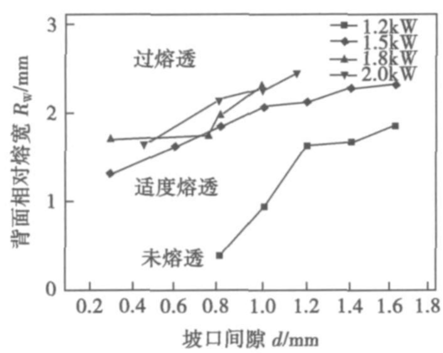

图 8 背面相对熔宽随坡口间隙的变化

Fig. 8 Variation of relative root width of weld with gap width

4 结 论

(1)通过调节激光功率、焊接电流或焊接速度增加焊接热输入,都可使背面熔宽和背面相对熔宽增大,从而改变熔透状态.

(2)一定工艺参数下,随着坡口间隙的增大,熔透状态从未熔透过渡到适度熔透,再过渡到过熔透.

参考文献:

[1] Claus B, Flemming O O. Review of laser hybrid welding[J]. Journal of Laser Applications, 2003, 17(1): 2−14.

[2] 张旭东, 陈武柱, 双元卿, 等. CO_2激光−MIG同轴复合焊方法及铝合金焊接的研究[J]. 应用激光, 2005, 25(1): 1−3. Zhang Xudong, Chen Wuzhu, Shuang Yuanqing, et al. Coaxial hybrid CO_2 laser-MIG welding system and its application in welding of aluminum[J]. Applied Laser, 2005, 25(1): 1−3.

[3] Petring D, Fuhmann C, Wolf N, et al. Investigations and applications of laser-arc hybrid welding from thin sheets up to heavy section components[C] // Proceedings of ICALEO. Florida, USA: LIA (Laser Institute of America), 2003, Section A: 1−10.

[4] Petteri J. Hybrid welding of hollow section beams for a telescopic lifter[C] // Proceedings of SPIE. Osaka, Japan: International Society for Optical Engineering, 2003, 4831: 353−356.

[5] Ishide T, Nayama M, Watanabe M. Coaxial TIG-YAG & MIG-YAG welding methods[J]. Welding International, 2001, 15(12): 940−945.

作者简介: 张永强, 男, 1978年出生, 博士, 高级工程师. 主要从事激光加工工艺及质量控制研究. 已发表论文 30余篇.

Email: zhyq01@gmail.com

somewhat increased and higher than cold rolled TiNi SMA base metal. The tensile strength of welded joint with post weld annealing treament achieves 63.6% of annealed TiNi SMA base metal and fracture strain achieves 82.5%. The phase change process of welded joint with post weld annealing treatment is almost the same with annealed base metal. When the welded joint of cold rolled TiNi SMA is annealed after welding, its phase change process is close to annealed base metal, and its shape memory effect is almost the same with annealed base metal.

Key words: TiNi shape memory alloy sheet; low power laser welding; shape memory effect

Evaluation method of penetration statuses in laser-MIG hybrid welding

ZHANG Yongqiang, CHEN Wuzhu, SHUANG Yuanqing, WANG Kangjian, SHAN Jiguo (1. Research Institute of Technology, Shougang Group, Beijing 100043; 2. Department of Mechanical Engineering, Tsinghua University, Beijing 100084). p 41-44

Abstract: The formation of weld root is an important criterion to evaluate the gap bridging ability and weld quality of hybrid welding in gapped butt welding. Therefore the concept of relative root width of weld was proposed as the criterion to evaluate penetration status in CO_2 laser-MIG hybrid welding. Base on relative root width of weld, the penetration statuses including moderate full penetration, partial penetration and excessive penetration were distinguished, and the effects of the variation of welding parameters and gap width on penetration status were further investigated. The results show that the relative root width can be increased by the change of welding parameters, and so the penetration status is changed. Under certain situation, as the gap width increases, the penetration status changes from partial penetration to moderate full penetration, and from moderate full penetration to excess penetration.

Key words: laser hybrid welding; evaluation criterion; penetration status; relative root width of weld

Effect of annealing treatment on formation of intermetallic phase in cold-sprayed Ni/Ti mechanical alloying coating

ZHOU Yong, YANG Guanjun, WANG Hongduo, LI Geng, LI Changjiu (1. State Key Laboratory for Mechanical Behavior of Materials, Xi'an Jiaotong University, Xi'an 710049, China; 2. School of Materials Science and Engineering, Xi'an Shiyou University, Xi'an 710065, China). p 45-48

Abstract: Three kinds of Ni/Ti mechanical alloying powder prepared by mechanical alloying at different milling time are employed to form Ni/Ti coatings by cold spraying. The microstructures of the coatings annealing under different conditions are characterized by scanning electron microscopy (SEM) and X-ray diffraction (XRD). It is found that the formation temperature of Ni-Ti intermetallics from the cold-sprayed alloy is decreased with increasing ball milling time for powder preparation. Moreover, the phase constitutions change from Ni_3Ti, B2-NiTi and Ti_2Ni to Ni_3Ti and Ti_2Ni. The increase of annealing temperature only leads to the change of the relative content of different intermetallic phases in the coating. The results show that intermetallic B2-NiTi phase formed during annealing exhibits good stability during cooling process.

Key words: cold spraying; mechanical alloying; annealing treatment; intermetallic compound

Weld fatigue life assessment based on fuzzy quality evaluation model

LI Xiangwei, ZHAO Wenzhong, ZHENG Chengde (1. School of Traffic and Transportation Engineering, Dalian Jiaotong University, Dalian 116028, China; 2. Technical Research Center of Qiqihar Railway Rolling Stock Co., Ltd., Qiqihar 161002, China). p 49-52

Abstract: The fuzzy comprehensive evaluation model of the welding quality is introduced based on the principle of fuzzy mathematics. According to GB3323-2005 standard, the weld quality classification factor set, the evaluation set and the weight vector are established, and fuzzy comprehensive evaluation is completed. In accordance with the principle of the largest degree of membership, the level of weld quality is determined, the livability of S-N curve have objective choice, so that the quantity of weld fatigue life is amended. Finally, by BS7608-1993 fatigue design and assessment of steel structures standard and actual example, the fuzzy evaluation model based on the quality of the weld fatigue life evaluation process is explained, and the results show that the model is feasible, the calculation results are reasonable.

Key words: weld quality; fuzzy evaluation; fatigue assessment

Design of digital control pulsed MIG arc welding power source

PANG Qingle (1. School of Information and Electronic Engineering, Shandong Institute of Business and Technology, Yantai 264005, China; 2. School of Computer Science, Liaocheng University, Liaocheng 252059, China). p 53-56

Abstract: Aiming at some of deficiencies in the control system with analogous control technology and single-chip control technology, such as poor flexibility, control precision and reliability, a control system based on a digital signal controller (DSC) and micro control unit (MCU) for pulsed metal inert gas (MIG) arc welding power source is designed, and the hardware circuit and software flow chart of the system are presented. In the system, DSC with the variable parameter PI control algorithm controls the arc voltage and welding current, and the parameters of PI controller are determined by an expert system in MCU. The real-time kernel of the μC/OS-II is reduced and ported in MCU, and multiple tasks including an expert system are designed. The experimental results show that the control system based on DSC and MCU for pulsed MIG arc welding power source has the advantages of quicker response, better reliability and more stable arc length.

Key words: pulsed metal inert gas welding; digital signal controller; micro control unit; PID control

Model of layer thickness of thin-walled parts in laser metal direct manufacturing

ZHU Gangxian, ZHANG Anfeng, LI Dichen, PI Gang (State Key Laboratory for Manufacturing Sys-